



SCIENTIA  
IRANICA

Sharif University of Technology

Scientia Iranica  
Transactions A: Civil Engineering  
www.scientiairanica.com



## Rotation capacity improvement of long link beams in eccentrically braced frames

B. Chegeni<sup>a,\*</sup> and A. Mohebkhah<sup>b</sup>

a. *Young Researchers Club, Khorramabad Branch, Islamic Azad University, Khorramabad, Iran.*

b. *Structural Engineering Division, Faculty of Civil and Architectural Engineering, University of Malayer, Malayer, Iran.*

Received 1 December 2012; received in revised form 23 September 2013; accepted 15 October 2013

### KEYWORDS

Eccentrically braced frame;  
Long link beam;  
Inelastic rotation capacity;  
Seismically compact sections;  
Stiffener.

**Abstract.** The use of short link beams in Eccentrically Braced Frames (EBFs) is generally preferred to long ones, mainly due to their high rotation capacity and energy dissipation under cyclic loadings. However, long links have the advantage of providing openings in the braced spans of EBFs. Based on a few tests conducted on long link behavior in the literature, Seismic Provisions (AISC-341-05) limits their rotation capacity to a small value of 0.02 rad. In this paper, a three dimensional finite-element model using ABAQUS is developed for the inelastic nonlinear analysis of long links to investigate their rotation capacity. It was found that using some new intermediate stiffeners, in addition to those specified in the Seismic Provisions, a large rotation capacity for long links can be achieved.

© 2014 Sharif University of Technology. All rights reserved.

### 1. Introduction

The concept of the Eccentrically Braced Frame (EBF) was proposed in the late 1970s and developed later by Popov and his co-workers ([1-5] among others) at the University of California, Berkeley (UCB). To have a ductile EBF, plastic hinges must be formed in specifically designed ductile link beams, while the other adjoining members (i.e. braces, columns and beams outside the link) remain in the elastic range. In other words, the links in an EBF act as structural fuses and dissipate earthquake-induced energy in a stable manner. To achieve this, based on the *capacity design concept*, adjacent members, which are presumed to be brittle and elastic, must be designed to have strength in excess of the maximum shear capacity of the link beams. Links with length less than  $1.6M_p/V_p$ , called short links, are dominated by shear web yielding.

Those longer than  $2.6M_p/V_p$ , called long links, are dominated by flexural yielding. Links with lengths between these limits, called intermediate links, experience both flexural and shear yielding simultaneously.

An important characteristic of the links in EBFs, to be considered structural fuses, pertain to their capability of withstanding inelastic rotation demands under cyclic loadings. The inelastic rotation capacity of long link beams has been given, based on previous experiments [5], and limited to a small value of 0.02 rad in the 2005 *AISC Seismic Provisions* for Structural Steel Buildings (AISC-341-05) [6]; hereinafter, referred to as *AISC Seismic Provisions*. The reasons for the small value of the long link rotation capacity given in *AISC Seismic Provisions* might be attributed to the following issues:

1. The loading protocol applied to the experiments by Engelhardt and Popov [5] was somewhat arbitrary and overly conservative, leading to small inelastic rotation capacities. The loading protocol for EBF links adopted in the 2005 *AISC Seismic Provisions* is based on the revised loading protocol developed

\*. *Corresponding author. Tel.: +98 851 2232346;*

*Fax: +98 851 2221977*

*E-mail addresses: b.chegeni@engineer.com (B. Chegeni);  
amoheb@malayeru.ac.ir (A. Mohebkhah)*

and proposed by Richards and Uang [7] for testing short links. Okazaki et al. [8] showed that short shear links tested by the revised loading protocol can achieve larger inelastic rotations than those currently considered in the 2002 *AISC Seismic Provisions* [9].

2. The experiments were conducted on long links attached to columns [5] having high axial forces, reducing their inelastic rotation capacities. Hence, it seems that links located within a span between two braces would be capable of developing high inelastic rotation capacity.
3. Some of the specimens' deterioration in strength was due to the initiation of severe flange buckling in the top flange of the brace connection panel [5]. It seems that using some properly detailed stiffeners, the observed deterioration in strength could be prevented, leading to high inelastic rotation capacity.
4. Failure in the link to column connections was the main factor in the onset of instability and the limitation of rotation capacity in most links tested by Popov. Since the rotation proposed by Popov was based on inappropriate pre Northridge connections, it seems that using the current connections (special connections proposed by Okazaki [10]) for the link next to the column, could lead to an increase in rotation capacity.

Few laboratory tests and numerical investigations have been conducted on the rotation capacity improvement of long links. Dusicka et al. [11] experimentally investigated the performance of built-up shear links designed from various plate steels. They concluded that the links designed without stiffeners using Low Yield Point (LYP) steel can reach high shear deformations of about 0.20 rad, exceeding the minimum limits outlined in current provisions, 0.08 rad. Della Corte et al. [12] used a finite element method to investigate the plastic overstrength of shear links. They found that three basic parameters: (i) axial forces, (ii) the ratio of flange over web area and (iii) the ratio of link length and cross section depth, have a combined effect on link shear overstrength. Also, they concluded that for very short links, with compact cross sections, values of shear overstrength up to 2 could be obtained. Daneshmand and Hosseini Hashemi [13] used an analytical model to investigate the behavior of intermediate and long link beams. They found that the rotation capacity of intermediate links is very sensitive to the slender ratio of the web.

Despite the aforementioned studies, new strategies have not been investigated to improve the rotation capacity of long links. The purpose of this paper is to investigate the significance of the aforementioned issues and the effectiveness of some proposed methods

on improving the inelastic rotation capacity of long flexural links in EBFs. For this purpose, a finite-element model, based on the commercial software package ABAQUS [14], is developed for the nonlinear inelastic analysis of long links located between two braces with different transverse stiffener patterns.

## 2. Nonlinear finite-element model

To investigate the inelastic behavior of long link beams, a nonlinear inelastic finite-element model is developed, based on the specifications and assumptions given in the following sections.

### 2.1. Mesh and material properties

The nonlinear computations were performed using the commercial finite element software package, ABAQUS [14]. ABAQUS has the ability to consider both geometric and material nonlinearities in a given model. Large displacement effects were accounted for by utilizing the nonlinear geometry option in ABAQUS. A 4-node doubly curved shell element with reduced integration, S4R [14], from the ABAQUS element library was used to model the web, the flanges and the intermediate stiffeners. The S4R element is suitable for complex plastic buckling behavior, has six degrees of freedom per node and provides accurate solutions for most relevant applications.

Dimensions and material properties of the specimens in this study are the same as Richards's dissertation specimens [15] in which cyclic coupon data from Kaufmann et al. [16] were used in calibrating the material model. The prototype material, designated as Steel C [16], was A572 grade 50 steel with yield strength of 54 ksi, and an ultimate strength of 72 ksi under monotonic testing.

### 2.2. Boundary conditions, cyclic loading and solution procedure

Since, in this study, the behavior of isolated link beams is investigated, boundary conditions are the same as proposed by Richard and Uang [17]. As can be seen in Figure 1, nodes on the left end were restrained against all degrees of freedom except horizontal translation. Nodes on the right end were restrained against all degrees of freedom except vertical translation. Transverse loading was applied as displacements to the right end nodes. These boundary conditions lead to constant shear along the length of the link, with equal end moments and no axial forces [17].

In order to take into account the deterioration in strength due to plastic local buckling, cyclic analysis was performed using the loading protocol given in Appendix S of the 2005 *AISC Seismic Provisions*. Monotonic analysis under-predicts buckling amplitudes and strength degradation [17]. This loading protocol requires that, after completing the loading cycle at a

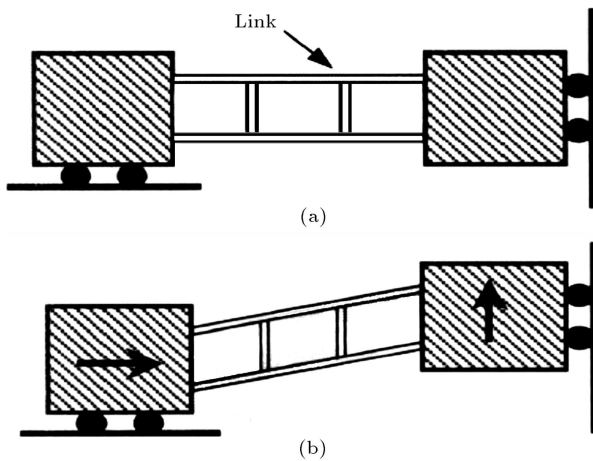


**Figure 1.** FEM model boundary conditions applied to the links: (a) Initial configuration; and (b) deformed configuration (as per Ref. [17]).

link rotation of 0.05 rad, the link rotation sequence be increased in increments of 0.02 rad, with one cycle of loading applied at each increment of rotation [6]. Link rotation was defined as the imposed transverse displacement divided by the link length. Although the loading protocol has been proposed for short shear links [7], the 2005 *AISC Seismic Provisions* [6] specifies no limitation for its usage. Hence, the loading protocol was used for all analyses in this paper.

### 3. Validation of the modeling technique

In this part, the accuracy of the finite element model of the link beams was investigated. The model was developed to simulate the performance of two links tested at the University of California, Berkeley (UCB), by Hjelmstad and Popov [3], and two A992 rolled shape links recently tested at the University of Texas, Austin (UTA) by Arce [18]. Boundary conditions, loading protocol, material properties and other details of modeling were the same as experimental conditions. Table 1 shows a comparison between maximum shear capacity obtained from the tests and the finite element analysis of all the specimens. It can be seen that agreement between experimental and numerical results is satisfactory with maximum error of 5% for specimen UCB 14. Figure 2 compares the deformed geometry

and hysteresis loops of the experimental specimen and the model for UTA 7.

### 4. Parametric study and discussion of results

After validating the finite element model, a parametric study was performed looking at the rotation capacity of long links made of built-up sections. The inelastic rotation capacity of the links is calculated as follows:

$$\gamma_p = \gamma_u - \gamma_e, \quad (1)$$

in which  $\gamma_u$  and  $\gamma_e$  are the ultimate and elastic rotation capacities, respectively. The ultimate inelastic rotation capacity was defined as the point where the hysteresis curve reduced below 80% of the ultimate shear capacity, as proposed by Richards and Uang [17].

To investigate the possibility of increasing the rotation capacity of the long links, two patterns using transverse stiffeners, in addition to those specified in the *AISC Seismic Provisions*, are studied in this study: (1) The use of stiffeners on one side placed at a distance of 0.75 times  $b_f$  from each end of the link, and (2) The use of diagonal stiffeners on one side within the link ends and the brace connection panels. Detailed discussion on the suitability of using each stiffener pattern is given in the following sections.

#### 4.1. The use of an additional stiffener at a distance of $0.75b_f$

In the first pattern, to investigate the possibility of increasing the rotation capacity of long links, besides the stiffeners at a distance  $1.5b_f$  from each end of the link, additional stiffeners were placed at a distance of  $0.75b_f$  on one side. Richards [15] conducted an analytical study to investigate the behavior and performance of 112 links, nine of which were long. In this study, those long links were simulated and analyzed with and without additional stiffeners (placed at a distance  $0.75b_f$ ) at the two ends. In addition, since specimen 7, which was tested in the Arce thesis [18], was similar to Richards's specimens in terms of dimensions and material properties, in this study, the behavior of specimens with and without additional stiffeners is investigated. Dimensions and material properties of these specimens are listed in Table 2.

**Table 1.** Comparison of maximum shear capacities obtained from experiment and finite element analysis.

| Specimen | Section  | $e_{(in)}$ | $e/(M_p/V_p)$ | $V_u(\text{EXP})$<br>(kip) | $V_u(\text{FEM})$<br>(kip) | Difference<br>(%) |
|----------|----------|------------|---------------|----------------------------|----------------------------|-------------------|
| UCB 4    | W18 × 40 | 28         | 1.16          | 207                        | 208                        | 0                 |
| UCB 14   | W18 × 35 | 36         | 1.91          | 184                        | 193                        | 5                 |
| UTA 7    | W10 × 33 | 73         | 3.4           | 73                         | 72                         | 1                 |
| UTA 9    | W16 × 36 | 48         | 2             | 173                        | 172                        | 0                 |

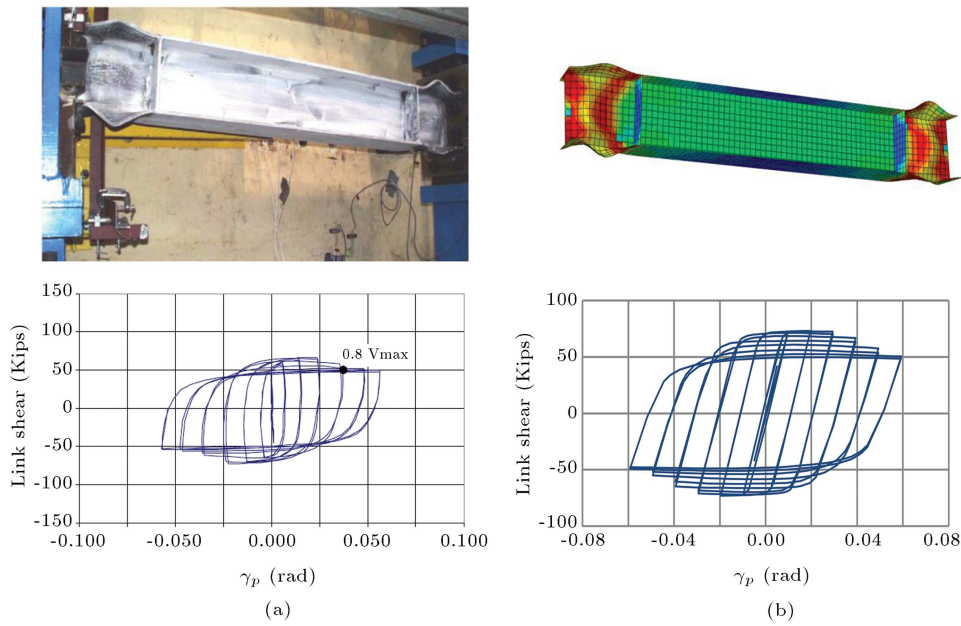


**Figure 2.** Deformed geometry and hysteresis curve of specimen UTA 7: (a) Test [18]; and (b) FEM analysis.

**Table 2.** Dimensions and material properties of long links.

| No                     | $d$<br>(in) | $t_w$<br>(in) | $t_f$<br>(in) | $b_f$<br>(in) | $e$<br>(in) | $\rho$ | $t_s$<br>(in) | $a$<br>(in) | $F_y$<br>(Ksi) | $F_u$<br>(Ksi) |
|------------------------|-------------|---------------|---------------|---------------|-------------|--------|---------------|-------------|----------------|----------------|
| 13 <sup>[15]</sup>     | 10.24       | 0.25          | 0.395         | 4             | 48          | 3.22   | 0.375         | 6           | 54.3           | 72.3           |
| 14 <sup>[15]</sup>     | 10.04       | 0.25          | 0.2           | 4             | 48          | 5.07   | 0.375         | 6           | 54.3           | 72.3           |
| 15 <sup>[15]</sup>     | 10.09       | 0.25          | 0.25          | 4             | 48          | 4.43   | 0.375         | 6           | 54.3           | 72.3           |
| 16 <sup>[15]</sup>     | 10.07       | 0.25          | 0.25          | 4             | 48          | 4.73   | 0.375         | 6           | 54.3           | 72.3           |
| 17 <sup>[15]</sup>     | 10.14       | 0.25          | 0.3           | 4             | 48          | 3.93   | 0.375         | 6           | 54.3           | 72.3           |
| 39 <sup>[15]</sup>     | 9.73        | 0.29          | 0.435         | 8             | 73          | 2.96   | 0.375         | 12          | 54.3           | 72.3           |
| 40 <sup>[15]</sup>     | 9.7         | 0.29          | 0.4           | 8             | 73          | 3.18   | 0.375         | 12          | 54.3           | 72.3           |
| 41 <sup>[15]</sup>     | 9.75        | 0.29          | 0.45          | 8             | 73          | 2.87   | 0.375         | 12          | 54.3           | 72.3           |
| 45 <sup>[15]</sup>     | 9.73        | 0.319         | 0.437         | 8             | 73          | 3.19   | 0.375         | 12          | 54.3           | 72.3           |
| 7 <sup>[18]</sup> Arce | 9.744       | 0.319         | 0.437         | 8             | 73          | 3.4    | 0.375         | 12          | 54.3           | 72.3           |

Since, in some specimens tested by Popov and Engelhardt [5], local buckling was observed in the flange of the beam in the brace connection panel, in some of these specimens, besides the link beam, the brace connection panels were also modeled at the ends of the link beams. Based on seismic provisions, lateral bracing was located at the two ends of the links to prevent lateral torsional buckling. Table 3 indicates the results of specimen analysis in which column 2 is the relative length of the links, and column 3 is the flange width-thickness ratio. Columns 4 and 5 are the calculated link rotation capacities, in the cases of without and with  $0.75b_f$  stiffeners, respectively. Column 6 is the rotation capacity of links having end brace connection panels with  $0.75b_f$  stiffeners, as shown in Figure 3. Columns 7 and 8 show the ultimate shear capacity of the specimens without and with additional stiffeners, respectively. Column 9 shows

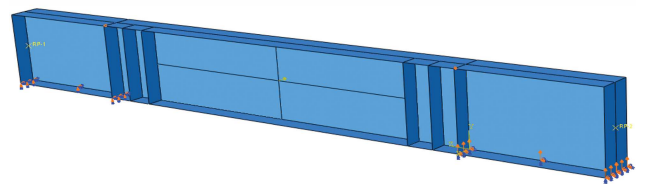


**Figure 3.** Geometry of the links along with the brace connection panels.

the rotation capacity of the specimens corresponding to the occurrence of top flange local buckling in the brace connection. Limitations of flange width-thickness ratios of specimens, for comparing the compactness of the specimens, are mentioned in Table 3. The sections with a flange width-thickness ratio less than  $\lambda_{ps}$  are called Seismically Compact sections; sections between  $\lambda_{ps}$  and  $\lambda_p$  are called Compact Sections, and sections between  $\lambda_p$  and  $\lambda_r$  are called Non Compact sections.

**Table 3.** Modeling results of long link with and without additional stiffeners at distance of  $0.75b_f$  at two ends of link.

| 1                  | 2      | 3      | 4                   | 5  | 6                                      | 7               | 8  | 9  |
|--------------------|--------|--------|---------------------|--|--|-----------------|--|--|
| No                 | $\rho$ | $b/2t$ | $\gamma_p$<br>(rad) | $\gamma_p$ (rad)<br>(with stiffener<br>$0.75b_f$ ) | $\gamma_p$ (rad)<br>( $0.75b_f$ -comb) | $V_u$<br>(kips) | $V_u$ (kips)<br>(with stiffener<br>$0.75b_f$ ) | $\gamma$ (rad)<br>(start of buckling<br>out of link) |
| 13 <sup>[15]</sup> | 3.22   | 5.06   | 0.08                | 0.08   | 0.08                                   | 60.4            | 61.3   | 0.08   |
| 14 <sup>[15]</sup> | 5.07   | 10     | 0.029               | 0.08   | 0.08                                   | 40              | 40.2   | 0.04   |
| 15 <sup>[15]</sup> | 4.43   | 8      | 0.026               | 0.08   | 0.08                                   | 45.1            | 45.89  | 0.05   |
| 16 <sup>[15]</sup> | 4.73   | 8.9    | 0.029               | 0.08   | 0.08                                   | 42.7            | 42.9   | 0.05   |
| 17 <sup>[15]</sup> | 3.93   | 6.665  | 0.049               | 0.08   | 0.08                                   | 50.7            | 51.3   | 0.06   |
| 39 <sup>[15]</sup> | 2.96   | 9.195  | 0.038               | -  | 71                                     | 71              | -  | -  |
| 40 <sup>[15]</sup> | 3.18   | 10     | 0.039               | 0.039  | -                                      | 66.5            | 66.5   | -  |
| 41 <sup>[15]</sup> | 2.87   | 8.9    | 0.048               | 0.046  | -                                      | 73              | 72.7   | -  |
| 45 <sup>[15]</sup> | 3.19   | 9.15   | 0.046               | 0.043  | -                                      | 72.9            | 72.8   | -  |
| 7 <sup>[18]</sup>  | 3.4    | 9.2    | 0.045               | 0.045  | -                                      | 72.4            | 72.6   | -  |

Seismic provisions slenderness limits for the used steel material:  $\lambda_r = 17.56$ ,  $\lambda_p = 8.78$  and  $\lambda_{ps} = 6.93$

Table 3 shows that seismically compact long links, with intermediate stiffeners at a distance of  $1.5b_f$ , can tolerate large rotation angles. However, rotation enhancement decreases with increasing the length ratio. Therefore, according to the data in Table 3, it is concluded that to seismically compact long links with a length ratio less than 4, and by using just one stiffener at a distance of  $1.5b_f$  at the end of the link, the rotation capacity can be increased up to 0.05 rad.

The results show that placing an additional stiffener at a distance of  $0.75b_f$  in the two ends, delays the occurrence of flange local buckling increasing the rotation capacity. This is true for links whose flange width is about half of the section depth, such as specimens 13-17. However, at the sections whose flange width is about the depth of the section, as specimens 39, 40, 41, 45 and specimen 7 Arce, these new stiffeners are not effective. This may be due to the fact that increasing the amount of  $b_f$  (flange width), enhances the distance of the intermediate stiffeners from the link ends. Therefore, bending plastic hinges are formed next to the link ends, and these stiffeners cannot be effective in preventing local buckling. Placing more stiffeners at two ends of the link (e.g. at a distance of  $0.375b_f$ ) shifts local buckling to the brace connection panels, so, it is not recommended.

As clear in Table 3, by modeling the brace connection panel, in sections which were not seismically compact like specimens 14, 15 and 16, local buckling was observed out of link (column 9) at a rotation of less than 0.08 rad. But, specimen 13, which was seismically compact, tolerated up to 0.08 rad with no local buckling out of the link. Despite the observed local buckling out of the link at the top flange in rotations of less than 0.08 rad, this local buckling led

to no reduction in rotation capacity, and the links that had an additional stiffener at  $0.75b_f$ , even though not a compact section, sustained a rotation of 0.08 rad (column 6).

For the long link specimen 17, despite having a seismically compact section, local buckling has been observed out of the link in a rotation of 0.06 rad. However, the ultimate shear capacity in the hysteresis loops did not dropped below  $0.8 V_u$  in this specimen too.

Therefore, according to the results, it can be concluded that by using one additional stiffener at a distance of  $0.75b_f$  at two ends of long links (with a relative length less than 3.5) at one side, whose flange width is about half of the section depth and which are seismically compact, a rotation capacity of 0.08 rad can be achieved (specimen 13), and specimens with too much relative length, and even with compact and non compact sections, can achieve more than 0.04 (specimens 14-17). It is also recommended that to delay the brace connection panel local buckling in these specimens, one partial depth stiffener with a 0.75 height of section depth should be welded to the top flange in a width of  $0.75b_f$  of the brace connection panels

However, it should be mentioned that these rotations might not be considered as the actual rotation capacity of long link beams. This is because the finite element models do not predict material failure and fracture, which generally occur in laboratory tests, causing loss of strength and consequently low rotation capacity. Therefore, the obtained rotation capacities should be validated through some experimental tests on long links.

Figure 4 shows the von Mises stress contour of specimen 13 with modeling of the brace connection

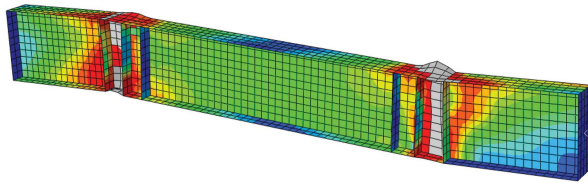


**Figure 4.** Von mises stress contour of specimen 13 at rotation 0.08 rad with modeling the brace connection panels.

panels at a rotation of 0.08 rad. As seen in Figure 4, because this specimen is seismically compact and has the proper relative length, no local buckling has occurred at the brace connection panels. However, it should be mentioned that the yielding observed in this place does not weaken the performance of the link. Popov and Engelhardt [5] have mentioned that this yielding, not local buckling, was, in fact, beneficial, as it contributed energy dissipation and reduced link inelastic deformation demands. In addition, it should be mentioned that maximum rotation applied to all specimens with and without additional stiffeners was 0.08 rad. So, it is obvious that the seismically compact specimen 13, with and without additional stiffeners, tolerates a rotation capacity of 0.08 rad.

**4.2. The use of diagonal stiffeners**

In the second pattern, the impact on rotation capacity when using two diagonal stiffeners at link ends (as shown in Figure 5(a)) was investigated. As can be seen, these stiffeners are embedded at a distance of  $1.5b_f$  at two ends of the link on one side and welded to the end stiffeners at a height of  $1/3$  of the section depth. In this section, to investigate the behavior of long links with this type of stiffener, all specimens considered in the above section are analyzed, with and without modeling the brace connection panels having diagonal stiffeners. The results of this modeling are listed in Table 4. To prevent penetration of the local buckling into the brace connection panel, the diagonal stiffeners are also placed in brace connection panels symmetrically with the same dimensions. Figure 5(b) shows a long link with two brace connection panels that has diagonal stiffeners in and out of the link. It should be mentioned that the thickness of the stiffeners are considered the same as the thickness of the internal stiffeners.

According to the results listed in Table 4, it was observed in the long links, in which flange width was about half of the section depth (e.g. specimens 13 to 17), in spite of their compactness or relative length limitations, using diagonal stiffeners would increase rotation capacity to 0.08 rad. Figure 6 shows specimen 14 with and without the diagonal stiffeners. In spite of its large length and non-compactness, by the use of diagonal stiffeners, the specimen could tolerate a rotation capacity of 0.08 rad with the ultimate shear capacity of more than  $0.8V_u$ .

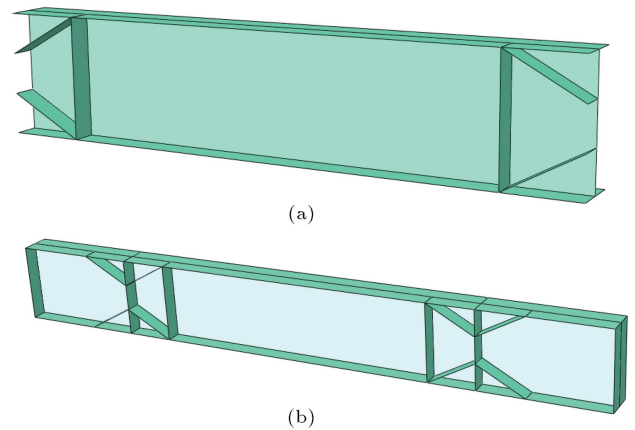


**Figure 5.** Using diagonal stiffeners at (a) link ends, and (b) link ends and brace connection panels.

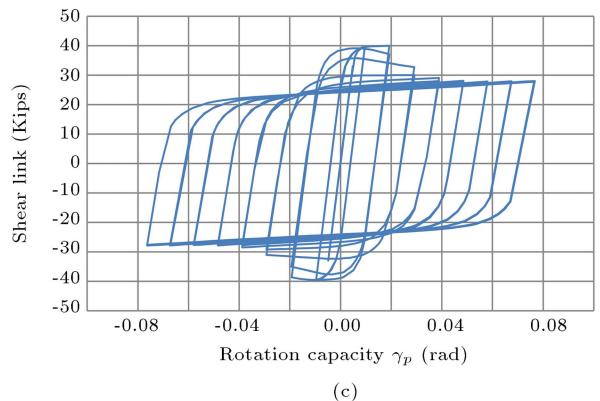
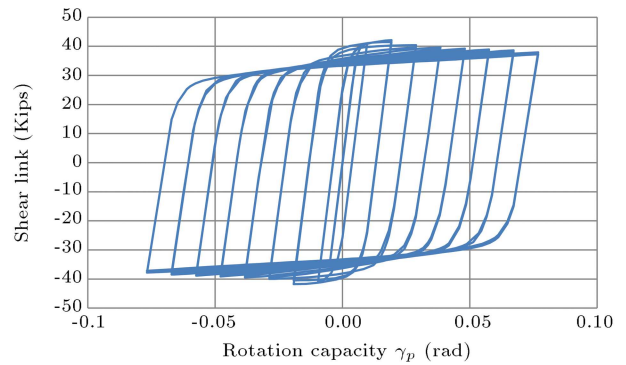
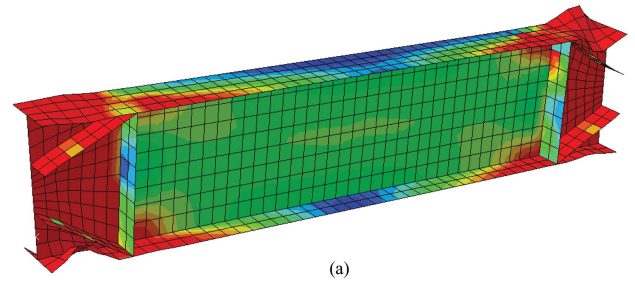


**Figure 6.** Specimen 14: (a) Von mises stress contour with diagonal stiffeners; (b) hysteresis loops with diagonal stiffeners; and (c) hysteresis loops without diagonal stiffeners.

**Table 4.** Results of long links with diagonal stiffeners.

| 1                  | 2      | 3      | 4                | 5   | 6                                   | 7            | 8   | 9   |
|--------------------|--------|--------|------------------|---|-------------------------------------|--------------|---|---|
| No                 | $\rho$ | $b/2t$ | $\gamma_p$ (rad) | $\gamma_p$ (rad)<br>(with diagonal stiffener) | $\gamma_p$ (rad)<br>(diagonal comb) | $V_u$ (kips) | $V_u$ (kips)<br>(with diagonal stiffener) | $\gamma$ (rad)<br>(start of buckling out of link) |
| 13 <sup>[15]</sup> | 3.22   | 5.06   | 0.08             | 0.08  | 0.08                                | 60.4         | 62.6                                      | N/A   |
| 14 <sup>[15]</sup> | 5.07   | 10     | 0.029            | 0.08  | 0.08                                | 40           | 41.9                                      | N/A   |
| 15 <sup>[15]</sup> | 4.43   | 8      | 0.026            | 0.08  | 0.08                                | 45.1         | 47.5                                      | N/A   |
| 16 <sup>[15]</sup> | 4.73   | 8.9    | 0.029            | 0.08  | 0.08                                | 42.7         | 44  | N/A   |
| 17 <sup>[15]</sup> | 3.93   | 6.665  | 0.047            | 0.08  | 0.08                                | 50.7         | 52.5                                      | N/A   |
| 39 <sup>[15]</sup> | 2.96   | 9.195  | 0.038            | 0.062   | 0.076                               | 71           | 72.9                                      | N/A   |
| 40 <sup>[15]</sup> | 3.18   | 10     | 0.039            | 0.064   | 0.068                               | 66.5         | 69  | N/A   |
| 41 <sup>[15]</sup> | 2.87   | 8.9    | 0.048            | 0.074   | 0.077                               | 73           | 75.1                                      | N/A   |
| 45 <sup>[15]</sup> | 3.19   | 9.15   | 0.046            | 0.063   | 0.067                               | 72.9         | 75.6                                      | N/A   |
| 7 <sup>[18]</sup>  | 3.4    | 9.2    | 0.045            | 0.63  | 0.08                                | 72.4         | 75.7                                      | N/A   |

Seismic provisions slenderness limits for the used steel material:  $\lambda_r = 17.56$ ,  $\lambda_p = 8.78$  and  $\lambda_{ps} = 6.93$

For investigation of the possibility of the transference of local buckling from the link to the brace connection panels, like the previous section, again, by modeling the brace connection panels at two ends of the link, all specimens were analyzed. Diagonal stiffeners were placed in brace connection panels symmetrical to internal diagonal stiffeners. Like Table 3, at Table 4, column 9 was considered for recording the rotations of the onset of local buckling in the brace connection panels. However, as can be seen in Table 4, using the diagonal stiffeners in the brace connection panels prevents the occurrence of local buckling in this region. Therefore, it is proposed that by using this type of stiffener at the long links, in which the flange width is half the section depth, without any limitations, a rotation capacity of 0.08 rad could be achieved.

Results presented in column 5 in Table 4 show that the use of diagonal stiffeners in the links whose flange width is about the section depth, like specimens 39 to 45 and 7 Arce, causes an increase in rotation until 0.06 rad. Although, according to the results in column 9 in Table 4, by modeling the brace connection panels, no buckling occurs in that region, the occurrence of local buckling at a distance of  $1.5b$  at two ends of the link led to a drop in the ultimate shear capacity in the hysteresis loops and a restriction of rotation capacities to the amounts listed in column 6. Therefore, it is proposed that using these types of stiffener in long links and brace connection panels, the wide flange sections, without sensitivity to the flange width-thickness ratio, could tolerate until 0.06 rad. As seen in Tables 3 and 4, these proposed stiffeners cause no significant increase in ultimate shear capacity and, thereby, in overstrength. Hence, for the design

of EBF's using this kind of stiffener, a conventional overstrength factor can be used.

For investigation of when not placing diagonal stiffeners in the brace connection panels, specimen 15, with brace connection panels, was modeled one time with two stiffeners at the top and bottom flanges at the brace connection panels, one time with only one stiffener at the top flanges and one time without any stiffener. As seen in Figure 7, if those two stiffeners were placed at the top and bottom flanges in the brace connection panel (Figure 7(a)), no local buckling occurred in the brace connection panels; even if one stiffener was placed in the top flange (Figure 7(b)), local buckling occurred. Therefore, in this type of stiffener, the brace under the bottom flange could not prevent local buckling, and a diagonal stiffener must be placed at the top and bottom flanges.

## 5. Conclusions

In this study, the nonlinear inelastic analysis of long links constructed of built up sections was studied using the finite element method. The main aim was to investigate the possibility of increasing the rotation capacity of long links and also to investigate the behavior of this type of link beam when increasing the numbers and changing the type of intermediate stiffener. It was found that the rotation capacity proposed by AISC2005 is not proper for all long links, and some links, according to the flange width-thickness ratio and relative length, could have more rotation capacity. Also, it was observed, by considering the number of stiffeners, the relative length, the flange width-thickness ratio and changing the type of stiffener, much rotation capacity could be achieved. However,

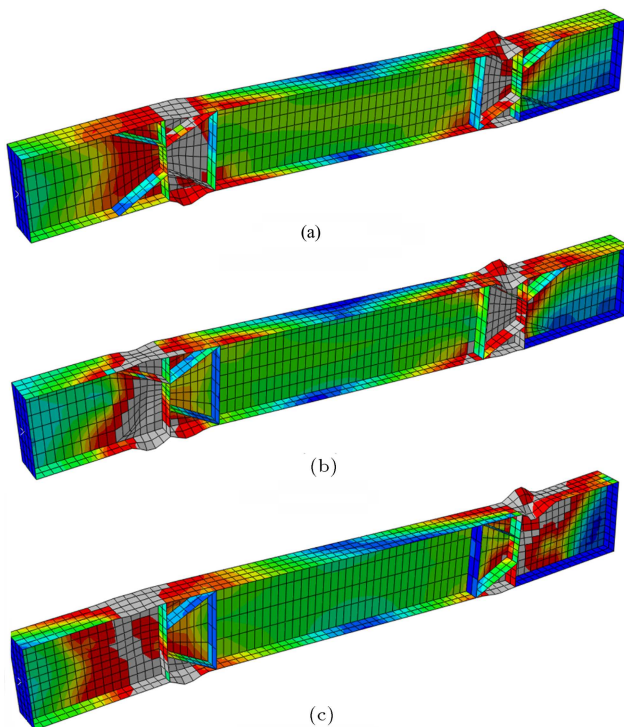


**Figure 7.** Combination of specimen 15 and brace connection panels: (a) with two stiffeners at top and bottom flange; and (b) with one stiffener at the top flange; and (c) without stiffener at brace connection panels.

owing to ignoring the effect of material failure in finite element modeling, observed high rotation capacities are not yet conclusive, and further experiment and study must be carried out to validate the results.

### Acknowledgement

The authors are grateful for the considerable assistance of Professor M.D. Engelhardt in providing documents regarding this research.

### Nomenclature

|            |   |
|------------|---|
| $A_w$      | Section web area  |
| $e$        | Link beam length  |
| $F_y$      | Yield stress of steel   |
| $F_u$      | Ultimate stress of steel  |
| $M_p$      | Section plastic moment capacity = $F_y Z$   |
| $Z$        | Plastic section modulus   |
| $V_n$      | Section nominal shear capacity<br>= $V_p = 0.6F_y A_w$  |
| $V_u$      | Section maximum shear capacity  |
| $\gamma$   | Total link rotation angle (ratio of the relative displacement of one ends of the link to the link length) |
| $\gamma_p$ | Link inelastic rotation capacity  |

|            |                                |
|------------|--------------------------------|
| $\gamma_e$ | Link elastic rotation capacity |
| $\Omega$   | Strain hardening overstrength  |
| $R_y$      | Material overstrength          |
| $\rho$     | Length ratio                   |

### References

1. Roeder, C.W. and Popov, E.P. "Eccentrically braced steel frames for earthquakes", *J. Struct. Div. ASCE*, **104**(ST3), pp. 391-412 (1978).
2. Malley, J.O. and Popov, E.P. "Shear links in eccentrically braced frames", *J. Struct. Eng. ASCE*, **109**(9), pp. 2275-2295 (1984).
3. Hjelmstad, K.D. and Popov, E.P. "Cyclic behavior and design of link beams", *J. Struct. Eng. ASCE*, **109**(10), pp. 2387-2403 (1983).
4. Kasai, K. and Popov, E.P. "Cyclic web buckling control for shear link beams", *J. Struct. Eng. ASCE*, **112**(3), pp. 505-523 (1983).
5. Engelhard, M.D. and Popov, E.P. "Experimental performance of long links in eccentrically braced frames", *J. Struct. Eng. ASCE*, **118**(11), pp. 3067-3088 (1992).
6. *AISC Seismic Provisions for Structural Steel Buildings* (AISC 340-05). Chicago (IL): American Institute of Steel Construction, March 9 (2005).
7. Richards, P.W. and Uang, C.M. "Cyclic development of testing protocol for links in eccentrically braced frames", *Proc. of the 13th World Conference on Earthquake Engineering*, Vancouver, Canada, Paper No. 2795 (2004).
8. Okazaki, T., Arce, G., Ryu, H.C. and Engelhardt, M.D. "Experimental study of local buckling, overstrength and fracture of links in eccentrically braced frame", *J. Struct. Eng. ASCE*, **131**(10), pp. 1526-1535 (2005).
9. *AISC Seismic Provisions for Structural Steel Buildings* (AISC 340-02). Chicago (IL): American Institute of Steel Construction, May 21 (2002).
10. Okazaki, T. "Seismic performance of link-to-column connections in steel eccentrically braced frames", Ph.D. Dissertation, Austin (TX, USA), Department of Civil Engineering, University of Texas at Austin (2004).
11. Dusicka, P., Itani, A. and Buckle, I.G. "Cyclic behavior of shear links of various grades of plate steel", *J. Struct. Eng. ASCE*, **136**(4), pp. 370-378 (2010).
12. Della Corte, G., Daniello, M. and Landolfo, R. "Analytical and numerical study of plastic overstrength of shear links", *Journal of Constructional Steel Research*, **82**, pp. 19-32 (2013).
13. Daneshmand, A. and Hosseini Hashemi, B. "Performance of intermediate and long links in eccentrically



- braced frames”, *Journal of Constructional Steel Research*, **70**, pp. 167-176 (2012).
14. *ABAQUS Standard User's Manual*. Hibbitt, Karlsson and Sorensen, Inc., Vols. 1, 2 and 3., Version 6.8-1. USA (2008).
  15. Richards, P.W. “Cyclic stability and capacity design of steel eccentrically braced frames”, PhD Dissertation, Univ. of California at San Diego, California (2004).
  16. Kaufmann, E.J., Metrovich, B.R. and Pense, A.W. “Characterization of cyclic inelastic strain behavior on properties of A572 Gr. 50 and A913 Gr. 50 rolled sections”, ATLSS Rep. No. 01-13, National Center for Engineering Research on Advanced Technology for Large Structural Systems, Lehigh Univ., Bethlehem, Pa. (2001).
  17. Richards, P.W. and Uang, C.M. “Effect of flange width-thickness ratio on eccentrically braced frames link cyclic rotation capacity”, *J. Struct. Eng. ASCE*, **131**(10), pp. 1546-1552 (2005).
  18. Arce, G. “Impact of higher strength steels on local buckling and overstrength of links in eccentrically

braced frames”, Masters Thesis, Univ. Texas, Austin, Tex. (2002).

## Biographies

**Behrouz Chegeni** is an MS degree graduate student at Malayer University, Malayer, Iran, where he is currently a member of the Young Researchers Club. His current research interests include buckling of structures, ductile design of structures and performance-based design.

**Amin Mohebkah** received his PhD degree, in 2007, from Tarbiat Modares University, Tehran, Iran, in the field of seismic design of masonry-infilled steel frames, and is currently Assistant Professor of Structural Engineering at Malayer University, Malayer, Iran. His research interests include ductile design of steel structures, buckling of thin-walled structures and seismic design of masonry structures.